JOURNAL OF MATERIALS SCIENCE 28 (1993) 5543–5547

Preparation of SiC–W_2C nano-composite powders by chemical vapour deposition of the SiH_4–CH_4–WF_6–H_2 system

LIDONG CHEN, TAKASHI GOTO, TOSHIO HIRAI
Institute for Materials Research, Tohoku University, Katahira 2-1-1, Sendai 980, Japan

SiC–W_2C composite powders were prepared by chemical vapour deposition (CVD) using SiH_4 + CH_4 + WF_6 + H_2 as source gases at a temperature of 1673 K. X-ray diffraction, TEM observation and infrared absorption were used to characterize the structures of the powders. The prepared powders consisted of SiC–W_2C composite particles and hollow β-SiC particles. The SiC–W_2C composite particles had a W_2C core and an SiC shell. The average particle diameters of the SiC–W_2C composite and hollow SiC particles increased from 18 to 30 nm and from 40 to 70 nm, respectively, with an increase of SiH_4 concentration. TEM and infrared spectrum analyses showed that the W_2C core diameter was unchanged (about 18 nm), while the SiC shell thickness varied from 1 to 6 nm with reaction conditions.

1. Introduction

Silicon carbide (SiC) and SiC-based composite materials are widely used in structural and electronic applications. The properties of SiC sintered bodies have been improved by dispersing nanometre-size components. These kinds of materials are called "nano-composites" [1–3]. The dispersion of a fine tungsten carbide (W_2C and/or WC) phase in SiC bodies is shown to be effective to improve the toughness [4, 5] or electric properties [6]. In the present work, powders containing SiC–W_2C nano-composite particles were prepared by chemical vapour deposition (CVD) using SiH_4, CH_4, WF_6 and H_2 as source gases. The deposition conditions and the structure of the powders were investigated.

2. Experimental procedure

The CVD reaction was carried out in a tube reactor at a total gas pressure (P_{tot}) of 0.1 MPa. A schematic diagram of the CVD apparatus is shown in Fig. 1. A mixture of CH_4 (99.99%), WF_6 (99.99%), H_2 (99.999%) and H_2–10.0 vol % SiH_4 (99.9999%) was used as the source gas. Since premature reactions between SiH_4 and WF_6 gases caused WSi_2 formation in the low-temperature region, the CH_4 + WF_6 + H_2 gases and SiH_4 + H_2 gases were separately introduced into the reaction tube. The SiH_4 + H_2 was introduced into the high-temperature region (~1000 K) using an alumina nozzle. The powders were synthesized at a reaction temperature (T_{dep}) of 1673 K and total gas flow rate (FR) of 3.3×10^{-5} m^3 s^{-1}. The volume fractions of source gases were [CH_4] = 12 mol %, [SiH_4] = 0 to 5 mol % and [WF_6] = 0 to 1 mol %.

The shape and structure of particles were examined by transmission electron microscope (TEM) (JEOL JEM-2000FX). An energy-dispersive X-ray spectrometer (EDX) (Tracor Northan TN5500-UTW) was used to measure Si and W contents. The KBr pellet method was adopted to obtain infrared (i.r.) absorption spectra using a spectrophotometer (Japan Spectroscopic IR-G) in the wave number range from 400 to 4000 cm^{-1}. The crystal structure was identified using an X-ray diffractometer (Rigaku RAD-IIB, nickel-filtered CuK_α). The contents of Si, C and W were determined by chemical analyses.

3. Results and discussion

Fig. 2 shows the X-ray diffraction pattern of the powder prepared at [SiH_4] = 4.5 mol % and [WF_6] = 0.5 mol %. The main phases were β-SiC and W_2C, and a small amount of WC was found. The ratio of β-SiC to W_2C increased with the increase of SiH_4 volume fraction ([SiH_4]).

Fig. 3 shows the effect of [SiH_4] on the composition of powders, SiC/(SiC + W_2C). No SiC was formed when [SiH_4] was below 1 mol %. The SiC content increased from 0 to 85 wt % as [SiH_4] increased from 1 to 4 mol %.

The equilibrium CVD diagram of the SiH_4–CH_4–WF_6–H_2 system is demonstrated in Fig. 4. This phase diagram was calculated by the optimization method [7] using the thermodynamic data [8, 9] of 51 gas species and eight solid species in the Si–C–W–H–F

0022–2461

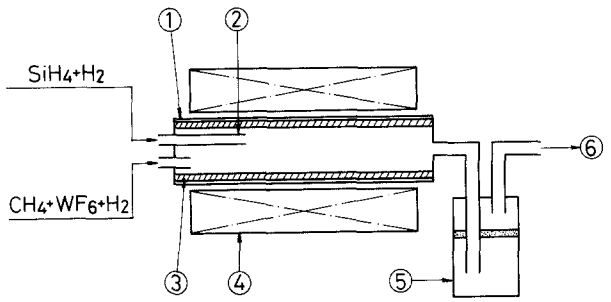

Figure 1 Schematic diagram of the apparatus for synthesizing SiC–W_2C nano-composite powder. (1) Mullite tube (internal diameter 35 mm), (2) Al_2O_3 nozzle, (3) RS–SiC tube (internal diameter 20 mm), (4) SiC resistance furnace, (5) collecting flask and filter, (6) gas outlet.

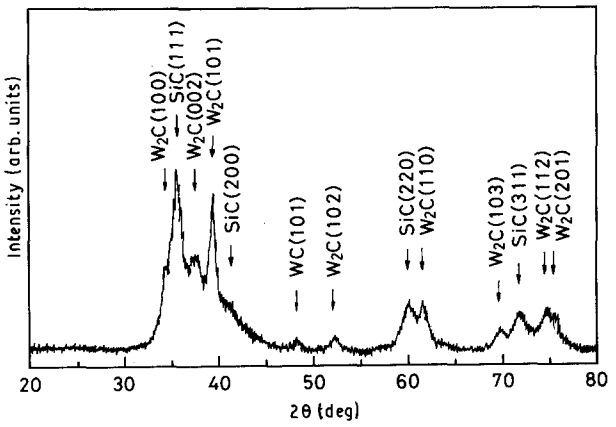

Figure 2 X-ray diffraction pattern of SiC–W_2C nano-composite powder prepared at $[SiH_4] = 4.5$ mol %, $[WF_6] = 0.5$ mol %, $[CH_4] = 12$ mol % and $T_{dep} = 1673$ K.

system (Table I). The shaded region in Fig. 4 indicates the present experimental conditions. The calculation suggests that β-SiC, W_2C and C phases should form under the present experimental conditions. Actually, β-SiC and W_2C were identified by X-ray diffraction as shown earlier, and a small amount of free carbon was detected by chemical analysis. However, when SiH_4 gas was introduced into the furnace entrance together with WF_6 gas, without the use of an alumina nozzle, the resulting powder consists mainly of WSi_2. The thermodynamic calculation also predicts the formation of WSi_2 below 800 K as shown in Fig. 4. Once WSi_2 had formed in the low-temperature region, it should be hardly carburized into SiC and W_2C by CH_4 in the high-temperature region, due to the kinetics.

Fig. 5 shows electron micrographs of the particles prepared at $[SiH_4] = 4.0$ mol % and $[WF_6] = 0.5$ mol %. Fig. 6 shows the electron diffraction patterns. The TEM observation distinguished two types of particle in the powder (type A and type B). The type A particles were hollow and were polycrystalline β-SiC in a single phase. The type-B particles had a shell–core structure and their electron diffraction pattern showed a mixture of β-SiC and W_2C.

Fig. 7 shows the EDX spectra of type A and type B particles which were from the same regions as those in

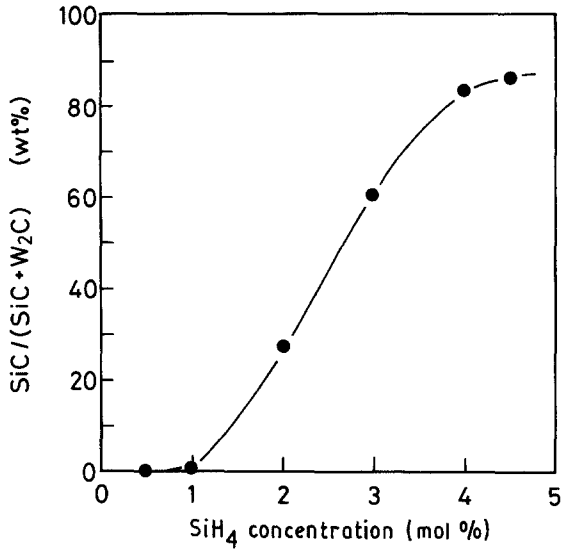

Figure 3 Effect of SiH_4 concentration on the chemical composition, SiC/(SiC + W_2C).

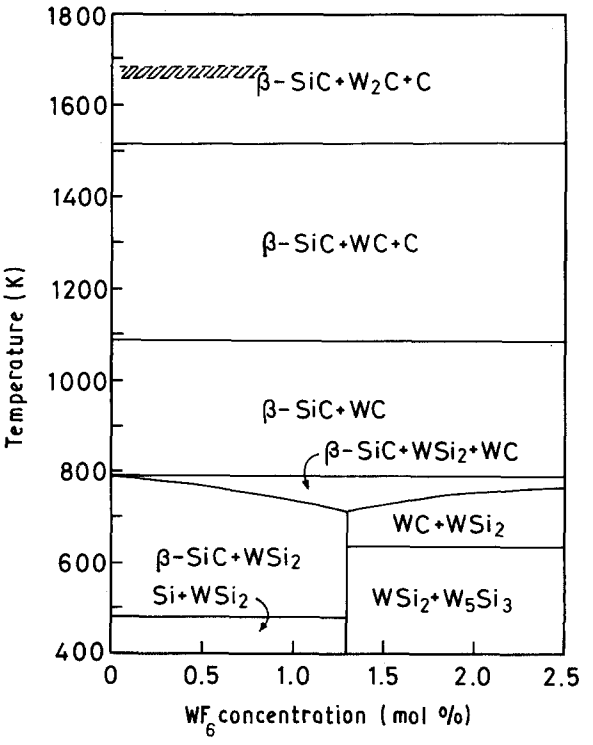

Figure 4 Calculated CVD phase diagram of $SiH_4 + CH_4 + WF_6 + H_2$ system. The shaded region refers to the present experimental conditions.

Fig. 5. The spectrum of commercial W_2C powder is also indicated in Fig. 7. Only Si (no W) was detected in type A, while type B particles had both Si and W. This result is in agreement with the earlier findings that type A is SiC and type B is SiC–W_2C composite.

The relations between SiH_4 volume fraction ($[SiH_4]$) and particle size for the type A and type B particles are shown in Fig. 8. The diameters of the hollow β-SiC particles increased from 40 to 70 nm, while those of SiC–W_2C composite particles from 18 to 30 nm with an increase of $[SiH_4]$. The diameters of hollow β-SiC particles are 2 to 3 times those of

TABLE I Chemical species in the Si–C–W–H–F system

Gas species									
H_2	H	Si	Si_2	Si_3	C	C_2	C_3	F	F_2
SiH	SiH_4	CH	CH_2	CH_3	CH_4	C_2H	C_2H_2	C_2H_4	F_2H_2
F_3H_3	F_4H_4	F_5H_5	F_6H_6	F_7H_7	SiF	SiF_2	SiF_3	SiF_4	CF
CF_2	CF_3	CF_4	C_2F_2	C_2F_4	C_2F_6	WF	WF_6	$SiHF_3$	SiH_2F_2
SiH_3F	CHF	CHF_3	CH_2F_2	CH_3F	C_2HF	$SiCH_3F_3$		SiC	Si_2C
SiC_2	$Si(CH_3)_4$								
Solid species									
Si	C	W	SiC	W_5Si_3	WSi_2	W_2C	WC		

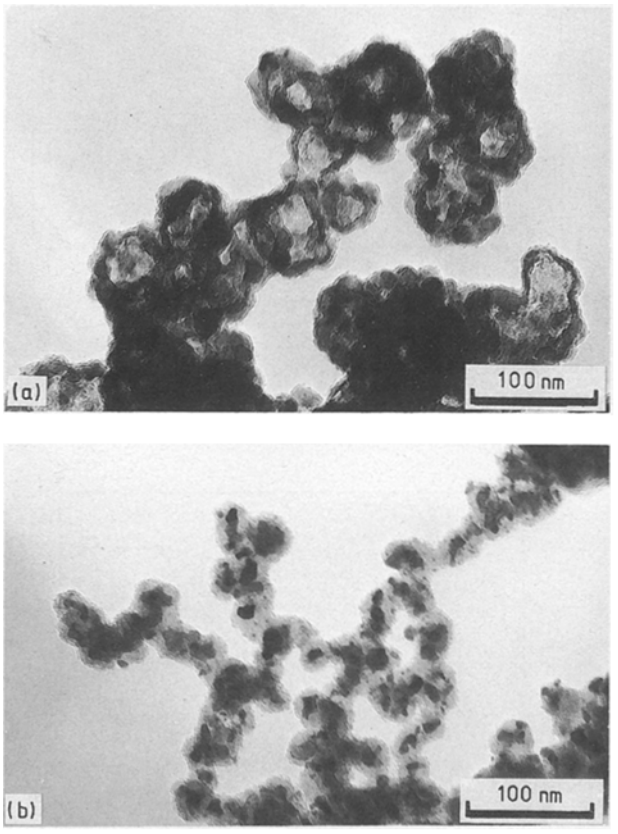

Figure 5 Electron micrographs of SiC–W_2C nano-composite powder prepared at $[SiH_4] = 4.0$ mol % and $[WF_6] = 0.5$ mol %: (a) hollow β-SiC particles (type A), (b) SiC–W_2C nano-composite particles (type B).

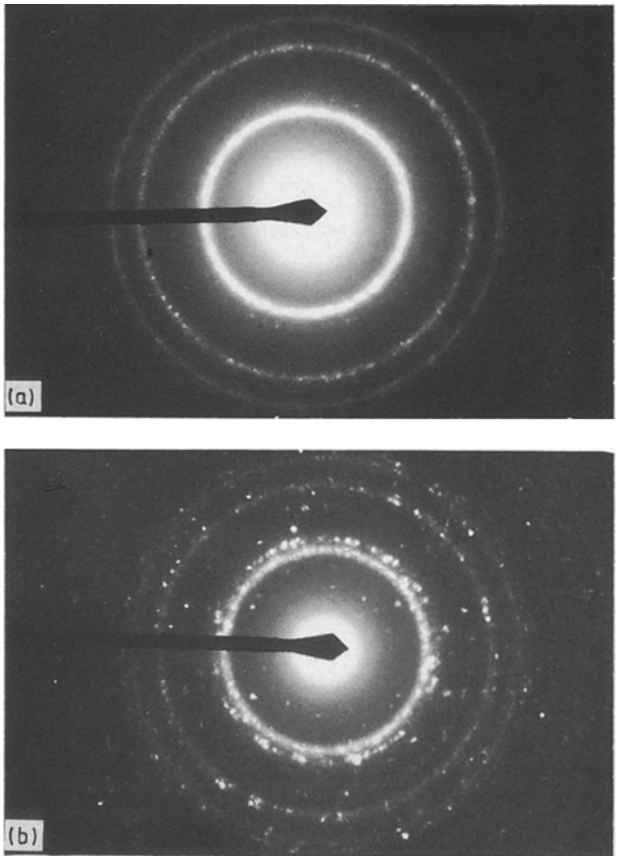

Figure 6 Electron diffraction patterns of the SiC–W_2C nano-composite powder illustrated in Fig. 5: (a) hollow β-SiC particles as in Fig. 5a, (b) SiC–W_2C nano-composite particles as in Fig. 5b.

SiC–W_2C composite particles. No hollow SiC particles were observed when $[SiH_4]$ was below 2 mol %.

Fig. 9 shows the i.r. absorption spectra of the powders obtained. The absorption spectrum of hollow SiC particles consists of a large peak at 830 cm^{-1} and a shoulder at 940 cm^{-1}. The mixtures of SiC–W_2C composite and hollow SiC particles had a larger shoulder at 940 cm^{-1}. The greater the amount of W_2C (i.e. the smaller the SiC amount), the larger the 940 cm^{-1} absorption shoulder. When the SiC amount was less than 60.5 wt % (Fig. 9d), one broad absorption peak centred at 890 cm^{-1} was observed.

The effective medium theory enables one to calculate the i.r. spectra [10, 11]. The absorption peak for the hollow SiC particles, by a surface phonon mode, should be theoretically located at 830 cm^{-1} with a shoulder at 940 cm^{-1} [11]. This calculation agrees well with the experimental results. For mixtures of the hollow SiC and SiC–W_2C composite particles, the absorption spectra have been contributed to by both types of particle. Two possibilities should be considered for the structure of the SiC–W_2C composite particles, i.e. either SiC(core) –W_2C(shell) or W_2C (core) –SiC(shell) structure. Since W_2C is electrically conductive, if the composite particles have an SiC(core)–W_2C(shell) structure, they should be conductive and thus inactive to infrared vibrations. In this case, the mixed powder would show the same infrared absorption behaviour as the hollow SiC particles. On the other hand, if the SiC–W_2C composite particles have an SiC(shell)–W_2C(core) structure, the effective medium theory on the surface phonon mode predicts that the infrared absorption behaviour will change with the SiC/W_2C content ratio and with the shell-/core size ratio of the SiC–W_2C composite particles. In fact, in the present work, the experimental infrared

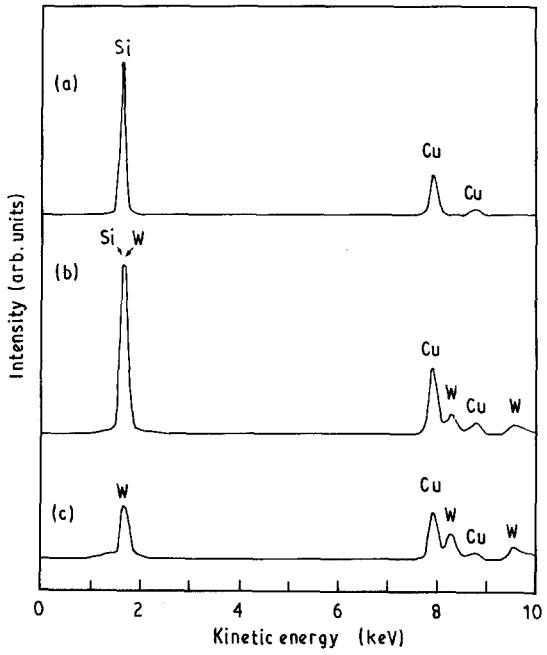

Figure 7 EDX spectra of SiC–W_2C nano-composite powder illustrated in Fig. 5 and W_2C standard powder: (a) hollow β-SiC particles as in Fig. 5a, (b) SiC–W_2C nano-composite particles as in Fig. 5b, (c) commercial W_2C standard powder.

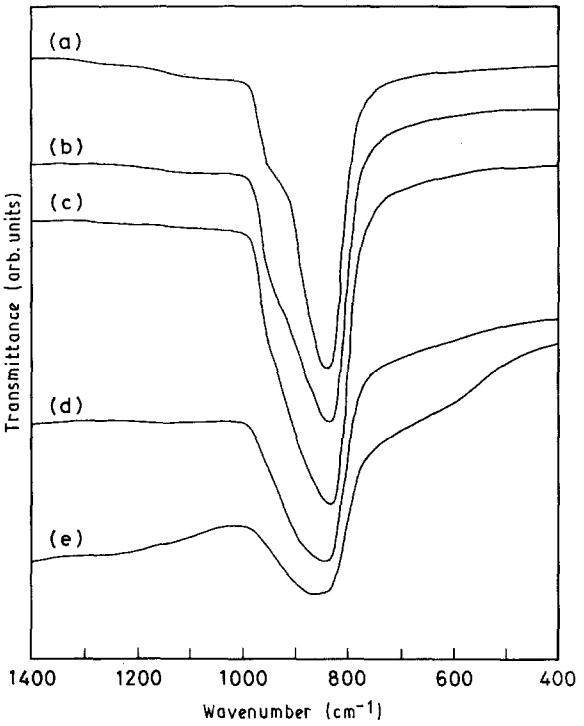

Figure 9 Infrared absorption spectra of (a) hollow SiC particles and (b–e) SiC–W_2C nano-composite particles: SiC/(SiC + W_2C) = (b) 90.0 wt %, (c) 83.3 wt %, (d) 60.5 wt %, (e) 27.4 wt %.

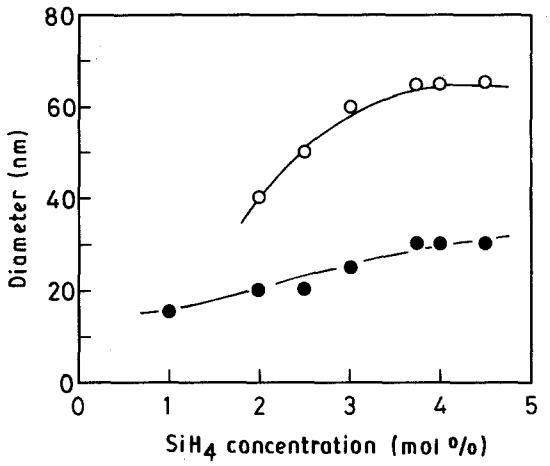

Figure 8 Effect of SiH_4 concentration on particle size: (○) hollow β-SiC particles corresponding to type A illustrated in Fig. 5a, (●) SiC–W_2C nano-composite particles corresponding to type B illustrated in Fig. 5b.

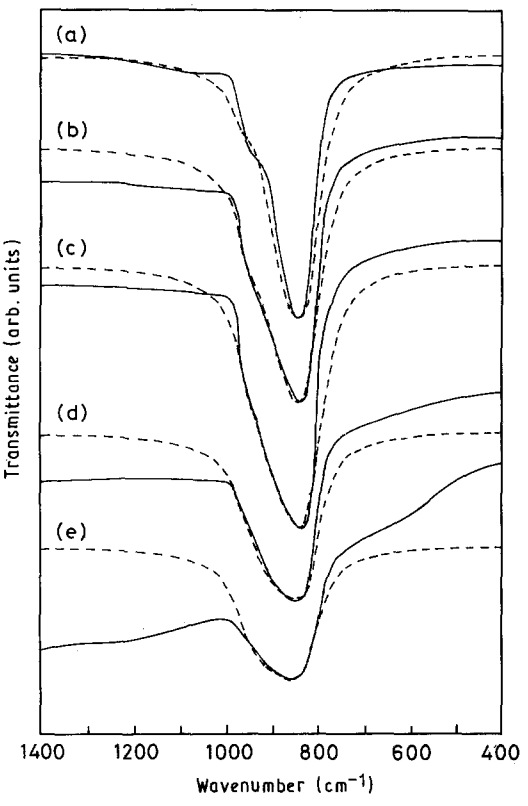

Figure 10 Comparison of (– – –) calculated and (——) measured infrared absorption spectra of (a) hollow SiC particles and (b–e) SiC–W_2C nano-composite particles corresponding to Fig. 9b–e, respectively.

spectra indeed changed with the SiC content (i.e. the particle sizes and the percentages of each type of particle) as is indicated in Fig. 9.

Under the assumption that the SiC–W_2C composite particles have an SiC(shell)–W_2C(core) structure, the infrared absorption spectrum calculations were examined. Fig. 10 compares the measured and calculated absorption spectra. The calculation details were reported elsewhere [11]. The particle diameters used in the calculation were shown in Fig. 8. The W_2C core diameter had a constant value at 18 nm. The SiC shell thicknesses were estimated from the difference between the core diameter and the outer diameter (particle size), which was 6 nm (Fig. 10b), 5 nm (Fig. 10c), 3 nm (Fig. 10d) and 1 nm (Fig. 10e). The smaller the SiC content, the larger and broader the absorption peak at 830 cm^{-1}, with a shift to higher frequencies. These calculated results agreed well with the present experiments. In the TEM observation (Fig. 5b), the core was darker than the shell. This suggests that a heavier element (i.e. W_2C not SiC) forms the core.

Therefore, the SiC–W_2C composite particles must have the SiC(shell)–W_2C(core) structure.

Hollow SiC particles were synthesized by CVD using the $SiH_4 + CH_4 + H_2$ system at 1673 K [12, 13]. The formation mechanism of hollow particles has been explained as follows: at first, Si particles form by the decomposition of SiH_4 at 900 to 1000 K, then the Si particles are carburized by CH_4. Si diffuses out from the core through the SiC layer leaving a hollow. WF_6 must decompose to form W at about 700 to 900 K [14, 15] much more easily than SiH_4 forms Si. If CH_4 gas is present in the atmosphere, W_xC ($x = 2$, 3) can be formed at 700 K [16, 17]. In the present experimental conditions, W_2C particles must have formed initially in the low-temperature region and Si deposited on the W_2C particles in the high-temperature region. The surface layer then reacted with CH_4 gas, forming an SiC shell. Finally, W_2C(core)–SiC(shell) nano-composite particles must have formed.

4. Summary

SiC–W_2C nano-composite powders were prepared by CVD using SiH_4, CH_4, WF_6 and H_2 as source gases at the reaction temperature of 1673 K. The structure and properties of the powders were investigated by TEM observation, i.r. absorption, EDX and X-ray diffraction. The powders were mixtures of SiC (shell)–W_2C(core) composite particles and hollow β-SiC particles. Thermodynamic calculations well explained the formation of SiC and W_2C phases. The W_2C core size was about 18 nm whereas the SiC shell thickness increased up to 6 nm with increasing SiH_4 concentration. The i.r. spectra of the powder containing the SiC–W_2C composite particles showed a peak at 830 cm^{-1} with a shoulder at 940 cm^{-1}. The peak became broader and shifted to higher frequencies as the W_2C content increased. These results were in agreement with calculations by the effective medium theory for the surface phonon mode of composite powders.

Acknowledgements

The authors would like to express their appreciation to Mr F. Chida for measurements of i.r. absorption spectra, and to Dr T. Sekiguchi and Miss S. Morita for EDX analysis.

References

1. T. HIRAI and T. GOTO, in "Tailoring Multiphase and Composite Ceramics", Materials Science Research Vol. 20, edited by R. E. Tressler, G. L. Messing, C. G. Pantano and R. E. Newnham (Plenum, New York, 1986) p. 165.
2. A. NAKAHIRA and K. NIIHARA, *Bull. Ceram. Soc. Jpn* **26** (1991) 218.
3. A. NAKAHIRA, K. NIIHARA and T. HIRAI, *J. Ceram. Soc. Jpn* **94** (1986) 767.
4. A. GOTO, T. MIYOSHI and H. KODAMA, Japanese Patent 61–101 466 (1986).
5. H. KODAMA and T. MIYOSHI, Japanese Patent 61–174 66 (1986).
6. K. TAKAHASHI, R. JIMBOU, Y. MATSUSHITA, S. YAMADA and T. KOSUGI, *J. Ceram. Soc. Jpn* **93** (1985) 123.
7. T. GOTO and T. HIRAI, *J. Chem. Soc. Jpn* **11** (1987) 1939.
8. D.R. STULL, and H. PROPHET (Eds), "JANAF Thermochemical Tables" 2nd Edn (US Government Printing Office, Washington, DC, 1971).
9. I. BARIN and O. KNACKE, (eds) "Thermochemical Properties of Inorganic Substances" (Heidelberg 1973, Supplements 1977).
10. K. YAMAMOTO, K. KIMURA, M. UEDA, H. KASAHARA and T. OKADA, *J. Phys. C, Solid State Phys.* **18** (1985) 2361.
11. L. CHEN, T. GOTO and T. HIRAI, *J. Mater. Sci.* **25** (1990) 4273.
12. *Idem, ibid.* **24** (1989) 3824.
13. Y. OKABE, J. HOJO and A. KATO, *J. Chem. Soc. Jpn* **2** (1980) 188.
14. W.A. BRYANT and G.H. MEIER, *J. Electrochem. Soc.* **120** (1973) 559.
15. W.A. BRYANT, *ibid.* **125** (1978) 1534.
16. Y. CHONG, N. WATANABE and N. TANAKA, *Kinzoku-Hyomen-Gijutsu* **36** (1985) 340.
17. N. WATANABE, T. TERADA, Y. CHONG and T. NAKAJIMA, *J. Chem. Soc. Jpn* **10** (1985) 1812.

Received 18 November 1991
and accepted 14 August 1992